Astronomy
&
Astrophysics

JEM-X observations of the Be/X-ray binary EXO 2030+375[⋆]

S. Martínez Núñez[1], P. Reig[1], P. Blay[1], P. Kretschmar[2,3], N. Lund[4], and V. Reglero[1]

[1] GACE, Instituto de Ciencias de los Materiales, Universidad de Valencia, PO Box 20085, 46071 Valencia, Spain

[2] Max-Planck-Institut für extraterrestrische Physik, Giessenbachstrasse, 85748 Garching, Germany

[3] INTEGRAL Science Data Centre, Chemin d'Écogia 16, 1290 Versoix, Switzerland

[4] Danish Space Research Institute, Juliane Maries Vej 30, 2100, Copenhagen, Denmark

Abstract. We have used data from the Joint European Monitor (JEM-X) to perform an X-ray spectral and timing analysis of the 42-s transient pulsar EXO 2030+375 during an X-ray outburst. X-ray pulsations are clearly detected with an average pulse period of 41.66 ± 0.05 s and an average pulse fraction of 60%. The profile of the energy spectrum did not change appreciably throughout the X-ray outburst, although the source shows a slightly softer spectrum during periastron passage in the energy range 9–25 keV. The 5–25 keV X-ray luminosity changed by a factor of 2 throughout the observations, reaching a maximum value of 3×10^{36} erg s^{-1}. These observations allowed us to verify the in-flight instrumental properties of the JEM-X Monitor.

Key words. INTEGRAL – JEM-X– BeX stars – HMXRBs – EXO 2030+375

1. Introduction

EXO 2030+375 belongs to the subclass of high-mass X-ray binaries known as Be/X-ray binary (Coe 2000 and references therein). In these systems a neutron star orbits around a Be star. Be stars are rapidly rotating B-type stars that show emission lines and infrared excess when compared to normal B-type stars. The line emission and the infrared excess are believed to be associated with a quasi-Keplerian disk formed by material flowing out from the Be star (Balona 2000 and references therein). The X-ray outbursts are produced when the neutron star accretes matter from the circumstellar disk.

When active, the X-ray flux of EXO 2030+375 is modulated by two types of periodic phenomena. 46-day outbursts are detected during periastron passage of the compact star (Wilson et al. 2002). These outbursts are known as type I outbursts and are characterised by moderate increases of the X-ray luminosity ($L_x < 10^{37}$ erg s^{-1}), low spin-up rates (if any) and recurrence at the orbital period. In addition to this long-term variation, the X-ray flux exhibits 41.7-s pulsations (Parmar et al. 1989; Reynolds et al. 1993; Reig & Coe 1998a), which are attributed to the rotation of the neutron star and results from the fact that the magnetic and rotation axis are misaligned.

Occasionally, Be/X-ray binaries also show giant outbursts (known as type II outbursts). During these outbursts the X-ray luminosity reaches near Eddington values ($L_x \sim 10^{38}$ erg s^{-1} for a neutron star). They do not correlate with the orbital phase and high spin-up rates are observed. For EXO 2030+375, only one giant outburst – the one that led to its discovery – has been so far reported (Parmar et al. 1989).

In common with other high mass X-ray binaries, the continuum spectral shape of EXO 2030+375 in the range 2–20 keV has been represented by a power law function ($\Gamma = 1.00 \pm 0.06$), an exponential cut-off ($\sim 8.85 \pm 0.33$ keV), coupled with a low-energy absorption ($N_H = 2.6 \pm 0.3 \times 10^{22}$ cm^{-2}) and an iron emission line at ~ 6.5 keV (Reig & Coe 1999).

The optical counterpart to EXO 2030+375 is a relatively faint (V=20) B0 Ve star (Motch & Jacot-Pacheco 1987; Coe et al. 1988), showing long-term optical and infrared variability (Reig et al. 1998b). The orbital parameters of the system can be found in Table 2 of Wilson et al. (2002).

In this paper, we have performed an X-ray timing and spectral analysis of EXO 2030+375 during a type I outburst, using data from the Joint European Monitor (JEM-X) on-board INTEGRAL.

2. Observations and data reduction

The data that have been analysed in this work were obtained during the INTEGRAL Performance and Verification phase (PV), which lasted from launch on October 17, 2002 to the end of December 2002. During this phase INTEGRAL was observing mostly the Cygnus X-1 region, performing

Table 1. EXO 2030+375 journal of observations.

Obs. number	SWID	IJD	Obs. time (s)	S/N	Orbital phase	counts/s	CL
1	001900100010	1 073.61300	1800	23.6	0.9876	3.17 ± 0.17	> 99%
2	001900110010	1 073.63503	1798	13.0	0.9881	1.96 ± 0.15	–
3	001900400010	1 074.27360	1796	29.1	0.0020	4.19 ± 0.18	>99%
4	001900580010	1 074.66973	1799	19.4	0.0106	2.47 ± 0.17	>99%
5	001900590010	1 074.69176	1797	16.8	0.0111	2.34 ± 0.14	<70%
6	001900900010	1 075.48207	1796	19.4	0.0282	3.46 ± 0.16	>99%
7	001900910010	1 075.50407	1796	20.9	0.0287	3.28 ± 0.18	>99%
8	002000060010	1 076.49525	3288	24.8	0.0502	3.38 ± 0.12	>99%
9	002000160010	1 076.71562	1783	13.4	0.0550	1.20 ± 0.16	∼ 70%
10	002000260010	1 076.93582	1773	23.7	0.0598	2.57 ± 0.16	∼ 99%
11	002000350010	1 077.13415	1776	30.7	0.0641	3.26 ± 0.13	>99%
12	002000360010	1 077.15594	1795	29.5	0.0646	3.53 ± 0.18	>99%
13	002000540010	1 077.55208	1795	38.3	0.0732	4.58 ± 0.18	>99%

different patterns of observations to check instrument be-
haviour and imaging performances.

The JEM-X monitor consists of two identical coded-
aperture mask telescopes co-aligned with the other instruments
onboard INTEGRAL. The detectors are microstrip gas cham-
bers with a collecting area of 500 cm^2 per unit located at a
distance of 3.4 m from the coded mask. JEM-X was designed
to work in the energy range 3–35 keV with an energy resolu-
tion of $\Delta E/E = 0.47 \times (E/1\,\mathrm{keV})^{-1/2}$ and a timing resolution of
122 μs. A detailed description of JEM-X can be found in Lund
et al. (2003).

A gas gain decrease (Lund et al. 2003) modified the low en-
ergy threshold of the detectors. The 50% efficiency level is now
reached at 4.2 keV, instead of the pre-launch value of 3.5 keV.
Above 25 keV, the quantum efficiency is determined by the
gradually diminishing absortion cross section of the Xenon gas
(at 25 keV, the efficiency is ∼35%). Therefore, for a relatively
weak source like EXO 2030+375, the optimum energy range
goes from 5 to 25 keV. Below 5 keV the electronic noise dom-
inates; above 25 keV, the background does.

An outburst of EXO 2030+375 took place during
December 9 to 17, 2002 corresponding to INTEGRAL orbit
revolutions 19 to 21. During these revolutions INTEGRAL ob-
served about 250 pointings in the Cygnus region, but in the
majority of these EXO 2030+375 is far from the JEM-X field
of view. Only in about 10% of the pointings was the source in-
side the JEM-X fully coded field of view. Another constraint is
the proximity of the two much stronger sources Cyg X-1 and
Cyg X-3. In many pointings the signal from these sources in-
creases the background for our source very significantly. As a
result, we have found only 13 pointings in which the source
was detected by JEM-X. These detections took place between
December 9–13, 2002, which correspond to revolutions 19
and 20 and orbital phases from 0.988 to 0.0732, according to
the ephemeris given by Wilson et al. (2002). This phase interval
corresponds approximately with the peak of the outburst. The
13 EXO 2030+375 detections are summarised in Table 1. We
give the Science Window Identifier (SWID), the INTEGRAL
Julian Date (IJD = JD–2 451 544.5), the observing time, the
signal-to-noise (S/N), the orbital phase, the count rate obtained

from the light curve extraction and the pulse period detection
confidence level (CL). Of these 13 detections, 3 were not con-
sidered due to a low signal to noise (Obs. 2) or instrumental
problems that are under investigation (Obs. 9 and 10).

The data reduction was carried out with the Offline
Scientific Analysis software, release 1.1, including those up-
dates which were available up to 2002 June 20, whereas the
data analysis was done using XSPEC and XRONOS pack-
ages. The latest response matrices (jmx1_rmf_grp_0004.fits and
jmx2_rmf_grp_0004.fits) have been used.

3. Results and discussion

3.1. Timing analysis

Figure 1 displays the JEM-X light curve of the entire observing
run (3.5 days) in the energy range 5 to 25 keV. The flux varies a
factor of 2 throughout the observations. For the sake of compar-
ison simultaneous RXTE, ISGRI observations and data from a
previous outburst detected by BATSE (Norton et al. 1994) are
also given. Note the shift of the outburst peak for Dec. 2002 ob-
servations with respect to the previous BATSE detection. This
shift has been seen in other outbursts. It has been attributed to
a global one-armed oscillation propagating in the Be star disc
(Wilson et al. 2002).

For all those observations with S/N greater than 19, we
can determinate the pulse period with a confidence level higher
than 99%. The average pulse period for those observations is
41.66 ± 0.05 s and the average pulse fraction is 60%. Figures 2
and 3 show the the time-averaged pulse profile and the power
spectrum of the best detection on 12th of December 2002
(SWID = 00200540010, Obs. 13). The straight line in Fig. 3
represents the 99% confidence level of detection for 1024 fre-
quencies (van der Klis 1989). The power spectrum was ob-
tained by performing a Fast Fourier Transform on the 1-s
binned light curve of Obs. 13. The normalization is given
by $2/N_{\mathrm{phot}}$, where N_{phot} is the total number of photons per trans-
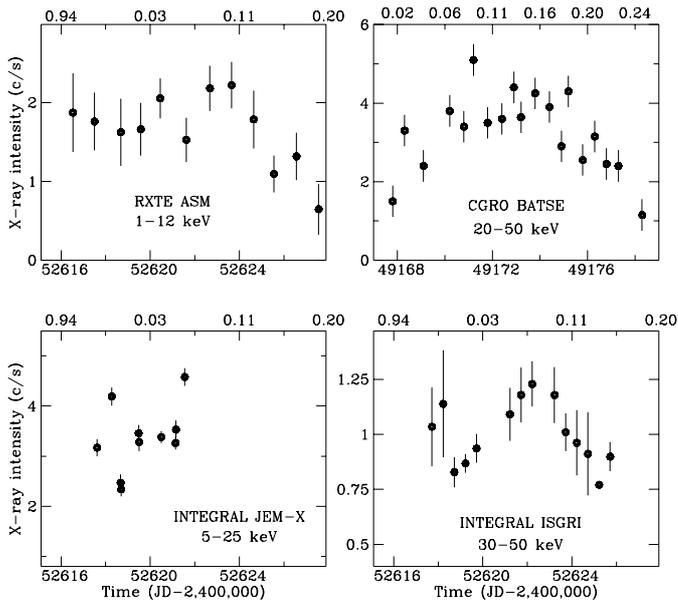form (Leahy et al. 1983; van der Klis 1989).

Fig. 1. Long-term light curve of EXO 2030+375 during the X-ray outburst. All light curves except that of CGRO BATSE (Norton et al. 1994) display simultaneous data. ISGRI data are normalized to the mean flux value.
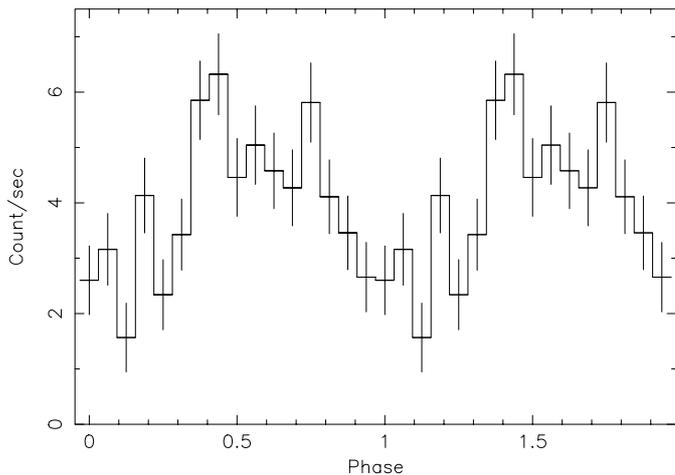

Fig. 2. EXO 2030+375 time-averaged pulse profile of the best detection, SWID = 002000540010.

3.2. Spectral analysis

In order to look for spectral shape changes throughout the X-ray outburst we first analysed all ten good JEM-X spectra separately. We tried different models to fit the energy spectra. Even though a single power law ($\Gamma \sim 2$) or an exponential ($E_c \sim 6$ keV) formally gave acceptable fits (reduced χ^2 lower than 2), the residuals present a well defined structure, indicating that a second model component is needed.

The inclusion of a moderate amount of absorption ($N_H = 2-3 \times 10^{22}$ cm^{-2}) does not improve the fit. As in the previous cases, the largest residuals occur below ~9 keV, indicating that absorption does not affect the spectrum at these relatively high energies (~4–9 keV). If we let the column density be a free parameter we obtain $N_H \approx 30 \times 10^{22}$ cm^{-2}, that is more than an order of magnitude larger than previous X-ray and
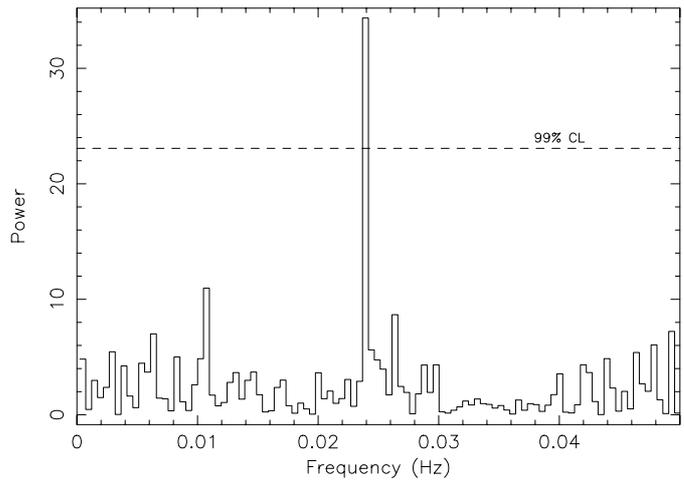

Fig. 3. EXO 2030+375 power spetrum for 1024 frequencies. The dashed line represents the 99% confidence level.
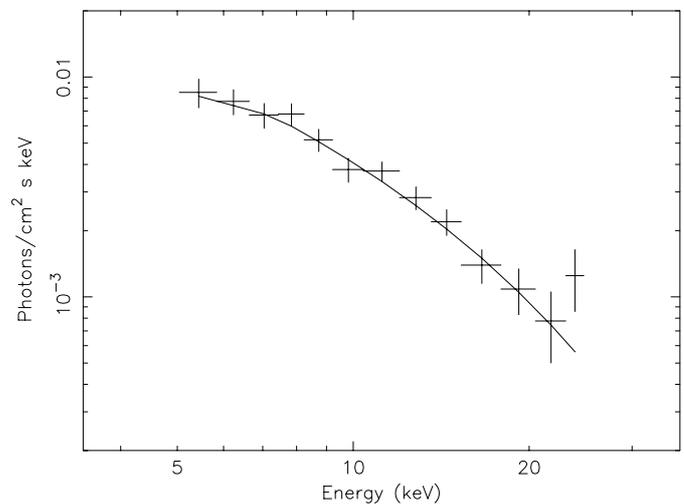

Fig. 4. Energy spectrum of observation 13 (SWID = 002000540010). The continuous line represents a powerlaw with a high energy cutoff.

optical observations, where the absorption was seen to vary in the range $2-3 \times 10^{22}$ cm^{-2} despite big changes in luminosity (Coe et al. 1988; Reynolds et al. 1993; Sun et al. 1994; Mavromatakis 1994; Reig & Coe 1999). The detection of an iron line at ~6.4 keV with moderate intensity (equivalent width ~200 eV) has been previously reported (Reynolds et al. 1993; Reig & Coe 1999). The relatively low signal to noise of the observations and the modest energy resolution of JEM-X prevent us from detecting the line in the JEM-X spectrum.

Restricting the spectrum to energies in the range 5–25 keV, the continuum can be fit with the canonical model for accreting pulsars, namely, a power law with an exponential cutoff at high energies. No significant differences are found among the different spectra. Figure 4 shows a representative energy spectrum. The average spectral parameters are given in Table 2. The photon index and cutoff energy agree with previous results (Reig & Coe 1999).

If each individual spectrum is fitted using a single power-law model in the energy range 9–25 keV, some marginal differences are found. Figure 5 shows the photon spectral index
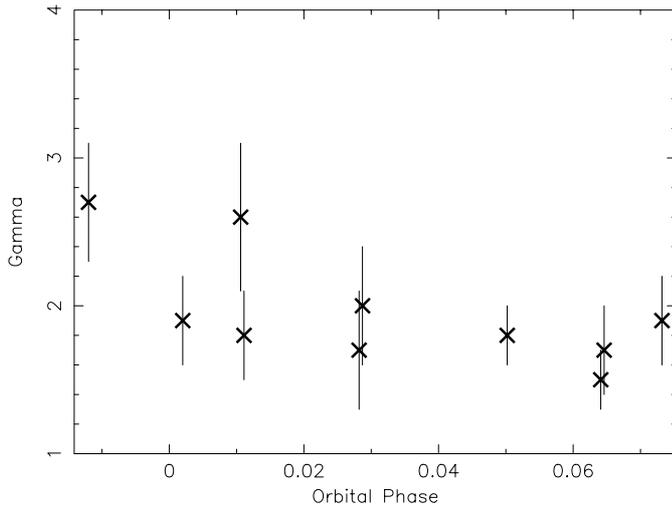
Fig. 5. Photon spectral index of the power law model in the energy range 9–25 versus orbital phase. Error bars are 1σ confidence region.

Table 2. Results of the spectral fit. Errors are within 90% of confidence level.

Parameter	Value
Γ	0.52 ± 0.12
E_c (keV)	7.8 ± 1.4
E_{fold} (keV)	10.0 (fixed)
Flux[a] (5–25 keV)	7.3
χ^2_{red}	1.46

[a] in units of 10^{-10} erg cm^{-2} s^{-1}

as a function of the orbital phase. At periastron passage the source shows a slightly softer spectrum than later in the orbit. The average value of the photon index for the first four observations is 2.4 ± 0.3, compared to 1.7 ± 0.2 at orbital phase larger than 0.02. This result is supported by the timing ISGRI and RXTE simultaneous data. As it can be seen in Fig. 1, the ISGRI light curve presents a maximum at 0.07 orbital phase, whereas no changes are seen in the RXTE data at the same phase.

The average X-ray luminosity in the energy range 5–25 keV was 2.1×10^{36} erg s^{-1} for an assumed distance of 5 kpc (Parmar et al. 1989). This value of the luminosity is of the same order as previous type I outbursts of this source. Reig & Coe (1999) found that the X-ray luminosity changed from ~9×10^{35} to ~4×10^{36} erg s^{-1} for a variation in orbital phase from 0.86 to 0.08 in the energy range 2.7 to 30 keV. This value is typical of Be/X-ray binaries during type I outbursts. The LS992/RX J0812.4-3114 is similar in this respect to EXO 2030+375.

LS992 shows 80-day periodic outbursts and X-ray pulsations with a pulse period of 31.88 s (Reig & Roche 1999; Corbet & Peele 2000) and variations in luminosity of 2–4 $\times 10^{36}$ erg s^{-1} (Corbet & Peele 2000).

4. Conclusion

The sensitivity of JEM-X allowed us to perform an X-ray timing and spectral analysis of the Be/X-ray binary EXO 2030+375 during an X-ray outburst. X-ray pulsations with a pulse period of 46.66 ± 0.05 s are clearly detected throughout the outburst. The average X-ray luminosity during the observations was 2.1×10^{36} erg s^{-1} in the energy range 5–25 keV. The results reported in this work confirms the performance requirements of JEM-X.

References

Balona, L. A. 2000, The Be Phenomenon in Early-Type Stars, ASP Conf. Ser., 214, 1
Coe, M. J., Longmore, A., Payne, B. J., & Hanson, C. G. 1988, MNRAS, 232, 865
Coe, M. J. 2000, The Be Phenomenon in Early-Type Stars, ASP Conf. Ser., 214, 656
Corbet, R. H. D., & Peele, A. G. 2000, ApJ, 530, L33, ApJS
Leahy, D. A., Darbro, W., Elsner, R. F., et al. 1983, ApJ, 266, 160
Lund, N., Brandt, S., Budtz-Joergensen C., et al. 2003, A&A, 411, L231
Mavromatakis, F. 1994, A&A, 285, 209
Motch, C., & Janot-Pacheco, E. 1987, A&A, 182, L55
Norton, A. J., Chakrabarty, D., Coe, M. J., et al. 1994, MNRAS, 271, 981
Parmar, A. N, White, N. E., Stella, L., Izzo, C., & Ferri, P. 1989, ApJ, 338, 359
Reig, P., & Coe, M. J. 1998, MNRAS, 294, 118
Reig, P., Stevens, J. B., Coe, M. J., & Fabregat, J. 1998, MNRAS, 301, 42
Reig, P., & Coe, M. J. 1999, MNRAS, 302, 700
Reig, P., & Roche, P. 1999, MNRAS, 306, 95
Reynolds, A. P, Parmar, A. N, & White, N. E. 1993, ApJ, 414, 302
Sun, X. J., Li, T. P., Wu, M., & Cheng, L. X. 1994, A&A, 289, 127
van der Klis 1989, Proc. NATO Advanced Study Institute Timing Neutron Stars
Wilson, C. A., Mark, H. F., Coe, M. J., Laycock, S., & Fabregat, J. 2002, ApJ, 570, 287